

# Role of Substrate Temperature on the Structural and Morphological Properties of ZnO Thin Films Deposited by Ultrasonic Spray Pyrolysis

Abdelkader DJELLOUL<sup>1</sup>, Khedidja BOUZID<sup>2</sup>, Fahima GUERRAB<sup>1</sup>

<sup>1</sup>*Laboratoire des Structures, Propriétés et Interactions Inter Atomiques,  
Centre Universitaire Khenchela-ALGÉRIE  
e-mail: djelloulabdelkader@yahoo.fr*

<sup>2</sup>*Laboratoire de microstructures et défauts dans les matériaux, Université de Constantine-ALGÉRIE*

Received 09.11.2007

## Abstract

Zinc oxide (ZnO) thin films have been prepared by ultrasonic Spray Pyrolysis (USP) technique using zinc acetate dihydrate dissolved in methanol, ethanol and deionized water. A thermodynamic analysis for the growth of ZnO thin films from zinc acetate and water vapor has been made. The evolution of the preferred crystalline orientations in the ZnO films was investigated systematically. The optical measurements reveal that films have a maximum transmittance of about 90% and a direct band gap of 3.26 eV.

**Key Words:** Zinc oxide, Ultrasonic spray pyrolysis, Thermodynamic study, X-ray diffraction, Optical properties.

## 1. Introduction

ZnO is amongst the most widely studied of all metal oxide systems and has recently become a very popular material due to its great potential for optoelectronics applications. The large direct band gap of 3.3 eV, along with the large exciton binding energy (60 meV) and many other advantages make ZnO a strong candidate for the next generation of ultraviolet light emitting diodes, a dye-sensitized oxide semiconductor solar cell [1], gas sensor [2], and lasing devices operating at high temperatures and in harsh environments [3, 4].

In this study, ZnO thin films have been prepared by USP technique, which involves spraying a zinc acetate solution onto a heated substrate. Zinc acetate ( $\text{Zn}(\text{CH}_3\text{COO})_2$ ) was first suggested as a potential single-source precursor by Tammenmaa et al [5] for ZnO film growth by atomic layer epitaxy. Highly oriented ZnO crystal thin films were obtained by the zinc acetate-H<sub>2</sub>O low pressure MOCVD system on glass substrates [6]. Only H<sub>2</sub>O fully oxidized the zinc acetate at substrate temperatures lower than 500 °C and produced a clean c-axis oriented ZnO film. Under isothermal conditions, the zinc acetate dihydrate loses its water of crystallization in a single step [7]. Anhydrous  $\text{Zn}(\text{CH}_3\text{COO})_2$  appeared at around 130 °C [8]. Arii et al concluded that the thermal process of crystalline  $\text{Zn}(\text{CH}_3\text{COO})_2$  formed directly crystalline ZnO by reacting with the introduced water vapor into the atmosphere. Thus, the reaction proceeded through single-step endothermic reaction without an intermediate [9].

In growing ZnO thin films, it is of primary importance to control the preferred orientation for each application. ZnO having the (0 0 2) orientation normal to the substrate is especially important for piezoelectric applications whereas the one with (1 0 0) orientation is of benefit to transparent conductive oxide applications [10–12]. The deposition conditions should be optimized for the particular application of interest in every case.

As demonstrated by the authors [5–9] noted previously, it is useful to perform a thermodynamic analysis of the principal reaction to identify the most favorable conditions for deposition of ZnO thin films by USP technique. The aim of this paper is to bring a contribution in this field, based some of our experimental results, from which some specific aspects of the growth processes can be extracted and discussed. In this respect we investigated the effect of substrate temperature on the resultant ZnO film properties. The preferred axis of orientation and residual involatile phases containing carbon contamination were used to determine the optimal deposition conditions for the growth of high-quality films.

## 2. Experimental Details

The solution used for the films investigated here had the following amounts: 2.2 g  $\text{Zn}(\text{CH}_3\text{CO}_2)_2 \cdot 2\text{H}_2\text{O}$  (Fulka 99.9%); 50 ml  $\text{H}_2\text{O}$  (deionized); 40 ml  $\text{CH}_3\text{OH}$  (Merck 99.5%); 60 ml  $\text{C}_2\text{H}_5\text{OH}$  (Merck 99.5%). A small amount of acetic acid (Acac) was added to aqueous solutions to adjust the pH value to about 4.8 to prevent the formation of hydroxides. Water is the most convenient oxidizing agent. Methanol and ethanol were the obvious choice because of their volatility and thus facilitating quick transformation of the precursor mist into vapor form, which is an important criterion for obtaining good quality films.

The ultrasonic spraying system used in this work consists of a commercial ultrasonic atomizer VCX 134 AT and substrate holder with heater. The ultrasonic vibrator frequency was 40 kHz and the power used was 130 W. The median drop size at 40 kHz is 45 microns. The nozzle to substrate distance was 5 cm and during the deposition, the solution flow rate was held constant at 0.07 ml/min. Our equipment can be divided in three parts connected between them. One bottle containing the zinc acetate solution, a perfusion system (a dropper chamber and a valve which regulates the dripping speed) and finally an ultrasonic atomizer (ultrasonic power supply, piezoelectric transducer and atomizing probe (nozzle)) located at 0.5 meter under the level of bottle. The zinc acetate solution is dispensed to the nozzle by gravity. To conserve the spray flow rate magnitude, the height of liquid was maintained constant by adding solution quantities, constantly, during deposition. The starting solution travels through the probe, and spreads out as a thin film on the surface. The oscillations at the tip disintegrate the liquid into micro-droplets, and then eject them to form a dense stream. Because the velocity of the droplets generated is very low, the probe is mounted with the tip facing downward in the direction of the substrate, and air disturbances kept to a minimum. Droplets impact on the heated substrate surface, spread into a disk shaped structure, and undergo thermal decomposition. The shape and size of the disk depends on the volume of the droplet, as well as the substrate temperature.

A dozen of ZnO thin films were deposited onto microscope cover glass substrates (dimensions, length  $\times$  width  $\times$  thickness: 30 mm  $\times$  12 mm  $\times$  1.2 mm) in the temperature range: 96 °C–434 °C and the deposition time was fixed at 30 min for all films. The substrate temperature was monitored with a thermocouple and controlled electronically.

The film morphology was examined using a (TS5130MM) scanning electron microscope (SEM). The compositional analysis of the selected areas was determined by an attached X-ray energy dispersive spectroscopy system (EDX). The structural analysis of the ZnO thin films is done by powder X-ray diffraction (XRD) data collected on Seifert XRD 3003-TT diffractometer using  $\text{CuK}_\alpha$  radiation.

The thickness of thin films was determined using a surface profiler (Dektak 3st). The transmittances of ZnO thin films were measured using a SpectroScan 80D uv-vis spectrophotometer in the 190–1100 nm spectral range.

### 3. Results and Discussions

The optical transmission spectra of ZnO films deposited on the glass substrate was recorded as a function of wavelength in the range 190–1100 nm and is shown in Figure 1. It was observed that, at 600 nm, the value of transmittance increases from 33% to 90% with the increase of the deposition temperature from 140 to 330 °C. Above 330 °C the value of transmittance decreases gradually with an increase of the substrate temperature. The transmittance of the film deposited at 350 °C and 434 °C was found to be 85% and 46%, respectively. According to the spectra of transmittance ZnO starts to appear at the substrate temperature of 140 °C which is good agreement with the measurements results obtained by Ariei et al [9].

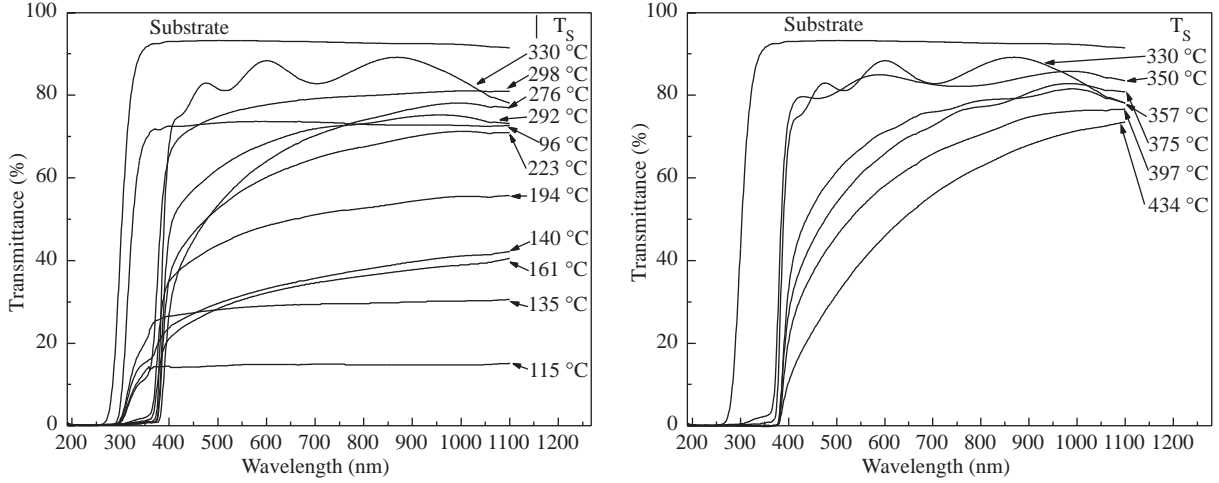
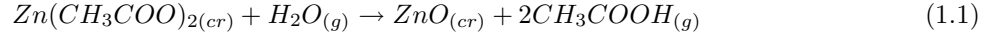


**Figure 1.** Transmission spectra of ZnO thin films deposited by USP technique on glass substrate at different  $T_S$ .

The reaction of zinc acetate with water vapor may be described by the equation



The reaction occurs at constant pressure  $P_t$  and constant temperature  $T_S$ . In a USP method, where only the substrate is heated, water vapor is produced at the substrate surface. In order to understand ZnO growth mechanisms, it is essential to determine the feasibility of the reaction (1) from the calculation of the thermodynamic equilibrium at a given set of processing conditions. However, due to the lack of thermodynamic data (entropy of solid zinc acetate), the calculations can not be obtained directly through the use of commercial packages. Thus, it has been almost impossible to calculate the Gibbs free energy changes for this reaction without the above thermodynamic data, which are the most important criteria to assess the possibility that the reactions will proceed. To solve this problem, the integral of the van't Hoff equation will be used and by means of the results of transmission spectra of ZnO thin films deposited by USP technique on glass substrate at different temperatures the constant of integration will be calculated.

The van't Hoff equation, which relates the equilibrium constants to the heat of reaction

$$\frac{d \ln K_p}{dT} = \frac{\Delta H}{RT^2}, \quad (1)$$

where  $R$  is the gas constant,  $T$  the absolute temperature and  $\Delta H$  is the change in enthalpy for the reaction. It is matter of experience that the enthalpy does not vary appreciably with the pressures of the substances concerned, and so  $\Delta H^\circ$  is replaced by  $\Delta H$  without specifying the conditions [13]. For exact calculations allowance must be made for the possible variation of the heat of reaction with temperature. The first step is the evaluation of  $\Delta_r H$  for the reaction (1). The thermochemical data for almost all reactive species interest are found in the literature [14–17] and are summarized in Table 1.

**Table 1.** Thermodynamic properties of some compounds interest taking part in reaction (1).

Species	Crystal			Gas		
	$\Delta_f H^\circ$ kJ/mol	$S^\circ$ J/mol·K	$C_p$ J/mol·K	$\Delta_f H^\circ$ kJ/mol	$S^\circ$ J/mol·K	$C_p$ J/mol·K
ZnO	-350.5	43.7	40.3			
Zn(C <sub>2</sub> H <sub>3</sub> O <sub>2</sub> ) <sub>2</sub>	-1079.9		153.6			
H <sub>2</sub> O				-241.8	188.8	33.6
CH <sub>3</sub> COOH				-432.2	283.5	63.4
	$C_{p(cr)}$ , J/mol·K			$C_{p(g)}$ , J/mol·K		
ZnO	49.06 + 5.11×10 <sup>-3</sup> T - 9.13 ×10 <sup>5</sup> T <sup>-2</sup>					
Zn(C <sub>2</sub> H <sub>3</sub> O <sub>2</sub> ) <sub>2</sub>	34.4 + 0.4T					
H <sub>2</sub> O				30.36 + 12.04×10 <sup>-3</sup> T + 4.11 ×10 <sup>5</sup> T <sup>-2</sup> -1429.9T <sup>-1</sup>		
CH <sub>3</sub> COOH				224.90 - 8.77×10 <sup>-3</sup> T + 127.88 ×10 <sup>5</sup> T <sup>-2</sup> -89561.53T <sup>-1</sup>		

The thermodynamic values of the enthalpy  $\Delta_f H_T$  as functions of temperature are as follows:

$$\Delta_f H_T(\text{ZnO}) = -368.42 + 49.06 \times 10^{-3}T + 2.55 \times 10^{-6}T^2 + 913T^{-1}$$

$$\Delta_f H_T(\text{Zn}(\text{CH}_3\text{COO})_2) = -1107.90 + 34.40 \times 10^{-3}T + 208.71 \times 10^{-6}T^2$$

$$\Delta_f H_T(\text{CH}_3\text{COOH}) = -416.03 - 69.57 \times 10^{-3}T + 54.43 \times 10^{-6}T^2 - 12.86 \times 10^{-9}T^3$$

$$\Delta_f H_T(\text{H}_2\text{O}) = -238.30 - 12.69 \times 10^{-3}T + 3.18 \times 10^{-6}T^2$$

where  $\Delta_f H_T$  are in kilojoules per mole. The variation of the change in enthalpy of the complete reaction (1) at the temperature is then given by

$$\Delta_r H_T = 145.72 - 111.79 \times 10^{-3}T - 100.47 \times 10^{-6}T^2 - 25.72 \times 10^{-9}T^3 + 913T^{-1}$$

where  $\Delta_r H_T$  are in kilojoules per mole. Putting  $\Delta_r H_T$  into equation (1) gives us the result

$$\frac{d \ln K_p}{dT} = \frac{17527}{T^2} - \frac{13.446}{T} - 120.85 \times 10^{-4} - 309.43 \times 10^{-8}T + \frac{109820}{T^3}, \quad (K^{-1}). \quad (2)$$

Now we shall consider the case of a maximum value for  $K_p$ . At the maximum point we have

$$\frac{d \ln K_p}{dT} = \left( \frac{\Delta H}{RT^2} \right)_{\max} = 0; \quad (\Delta H)_{\max} = 0; \quad T_{\max} = 736 \text{ K}.$$

At temperature of 736 K the reaction (1) ceases in its current form. When heated above 440 °C, acetic acid decomposes to produce carbon dioxide and methane, or to produce ketene and water.

According to the spectra of transmittance (Figure 1), ZnO starts to appear at the temperature of 140 °C. Thus, at 413 K,  $\ln(K_p) = 0$ . General integration of the van't Hoff equation (2), where the constant of integration is found to be 129.01, gives the equilibrium constant for reaction (1) in the form

$$\ln K_p = -\frac{17527}{T} - 13.446 \ln T - 120.85 \times 10^{-4}T - 154.72 \times 10^{-8}T^2 - \frac{54910}{T^2} + 129.01.$$

Thus, knowledge of  $K_p$  allows prediction of the relative proportions of products and reactants in a reaction. In the calculation, a reaction condition is specified by  $T_S$ , partial pressure of H<sub>2</sub>O and Acac. The equilibrium partial pressures of the gaseous species can be via the relation

$$p_{Acac} = \sqrt{K_p p_{H_2O}}.$$

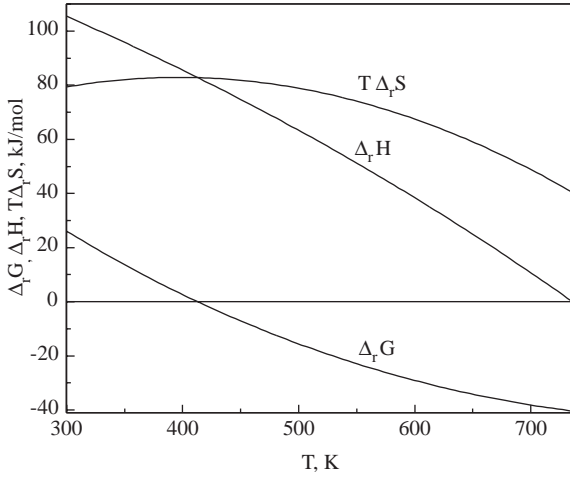
The ratio of the partial pressure of one component of a gas to the total pressure is:

$$X_i = \frac{p_i}{P_t},$$

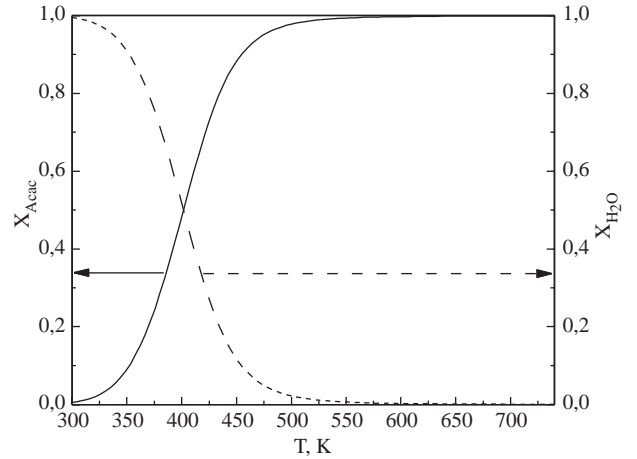
where  $X_i$  is the mole fraction of gaseous species  $i$ .

Figure 2 shows the calculated Gibbs free energy, enthalpy and  $T\Delta_r S$  change of the reaction (1) as a function of temperature. Gibbs free energy ( $\Delta_r G_T = -RT \ln(K_P)$ ) decreases gradually with an increase of the reaction temperature and will become zero at 413 K. It will become negative above 413 K, which suggests that the reaction can now proceed normally. The equilibrium constant of the reaction is 431.26 at 621 K, which means that a significant conversion of the reactant will be expected. However, the positive Gibbs free energy change suggests that the reaction cannot proceed at  $T_S < 413$  K. It can be concluded that the reaction of the growth of ZnO thin films from zinc acetate and water vapor is possible thermodynamically at temperature higher than 140 °C.

Figure 3 shows the temperature dependence of mole fraction of acetic acid and water vapor. At fixed total pressure, with increasing  $T_S$ ,  $X_{Acac}$  increase while  $X_{H_2O}$  decreases, which reflects the fact that reaction (1) is endothermic. When  $T_S$  is above 348 °C, the principal gas species is Acac and its molar fraction approaches a value approximately equal to 1 (solid line). These data clearly confirm the consumption of water vapor and release of acetic acid vapor at the end of the reaction during the process of growth.



**Figure 2.** Variation of the Gibbs free energy, enthalpy and  $T\Delta_r S$  change of the reaction (1) with temperature.



**Figure 3.** Temperature dependence of mole fraction of acetic acid and water vapor.

X-Ray diffraction analysis, obtained for  $2\theta$  scans between  $20^\circ$  and  $70^\circ$ , indicated that the deposited ZnO films on the glass substrate were polycrystalline and retained a hexagonal structure type wurtzite. The diffraction peaks are easily indexed on the basis of the hexagonal structure of ZnO ( $P6_3/mc$ ,  $a = 3.249 \text{ \AA}$ , and  $c = 5.205 \text{ \AA}$ , JCPDS 05-0664).

To better understand the decomposition process during USP, a set of samples were deposited at temperatures between 194 and 415 °C. Figure 4(a), (b) shows the XRD patterns and SEM micrographs (b) of ZnO films. The results show that the thin films grown at  $T_S = 320$  °C is crystalline since diffraction peak appears in the spectrum corresponding to the strong (1 0 0) and weak planes of the ZnO phase and three extra peaks which possibly originates from the presence of residual involatile organic compounds. These films have usually contained large amounts of organic compounds resulting from incomplete decomposition of the metal-organic source (zinc acetate) [18].

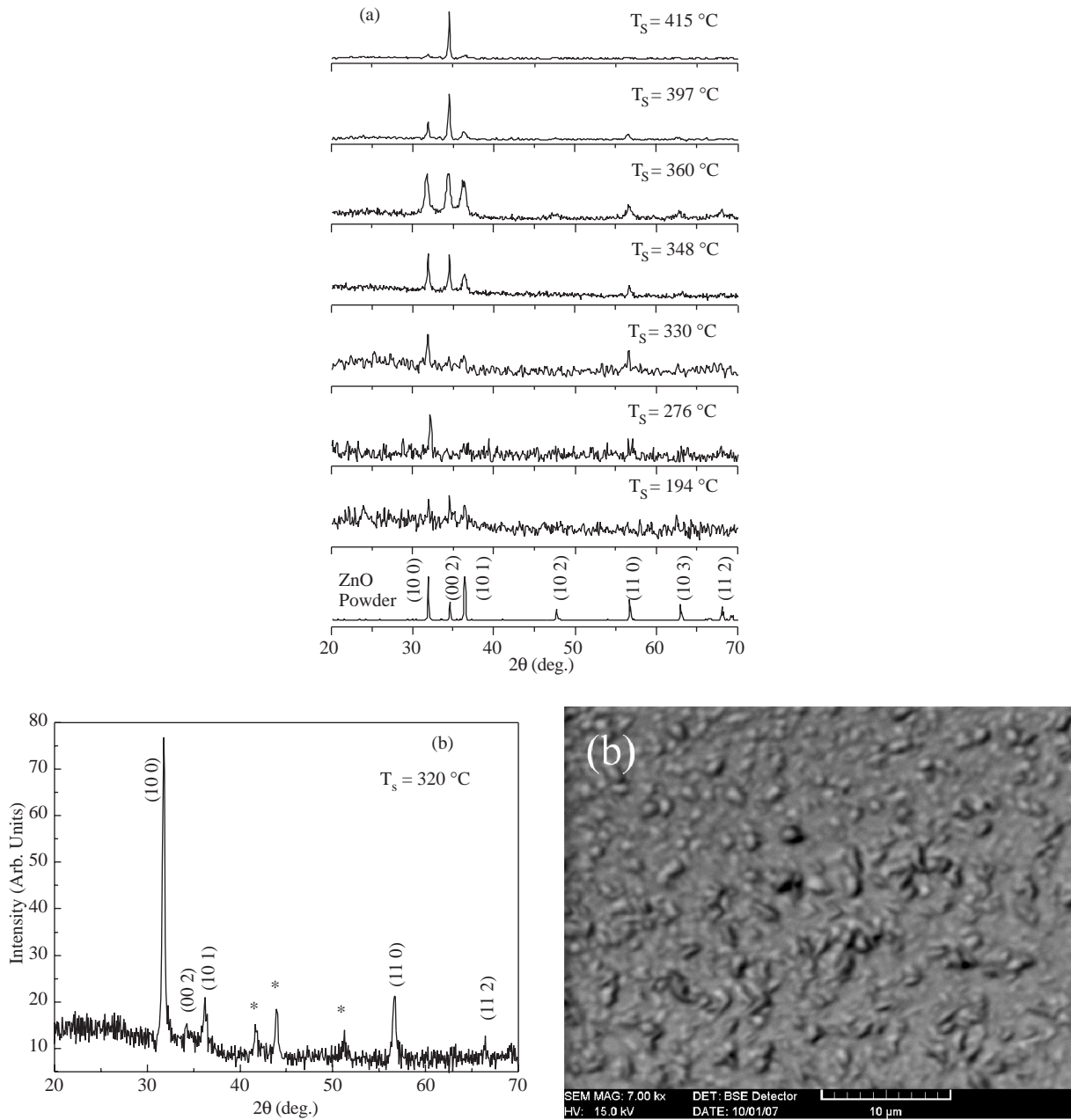


**Figure 4.** (a) X-ray diffraction patterns for ZnO films deposited at different substrate temperatures and ZnO powder, (b) XRD patterns and SEM micrographs for ZnO films deposited at  $T_S = 320$  °C, (\*indicates extra peaks).

From Figure 4(a), it is seen that the reflections for the parent residual organic compounds disappear completely, whereas the (1 0 0), (0 0 2), (1 0 1) and (1 1 0) reflections for hexagonal ZnO show up. The films exhibit strong (1 0 0) orientation when  $T_S \leq 348$  °C. When the  $T_S$  exceeds 348 °C, other peaks such as (1 0 0), (0 0 2), and (1 0 1) also develop stronger. Raising  $T_S$  changed preferred orientations from (1 0 0) to (0 0 2) with an intermediate stage, which is a powder like structure. It is clear from the Figure 4(a) that as  $T_S$  is increased the thin films adopts a preferred orientation, with the  $c$ -axis (0 0 2) perpendicular to the substrate. In order to explore the dependence of structural properties on the substrate temperature, we investigated the changes in structural characteristics such as the crystal structure and surface morphology by means of XRD and SEM. Figure 5(a–c) shows three XRD patterns and SEM micrographs of the films

grown at 306, 350 and 406 °C to illustrate the surface morphology of the ultrasonic sprayed films deposited at different temperatures.

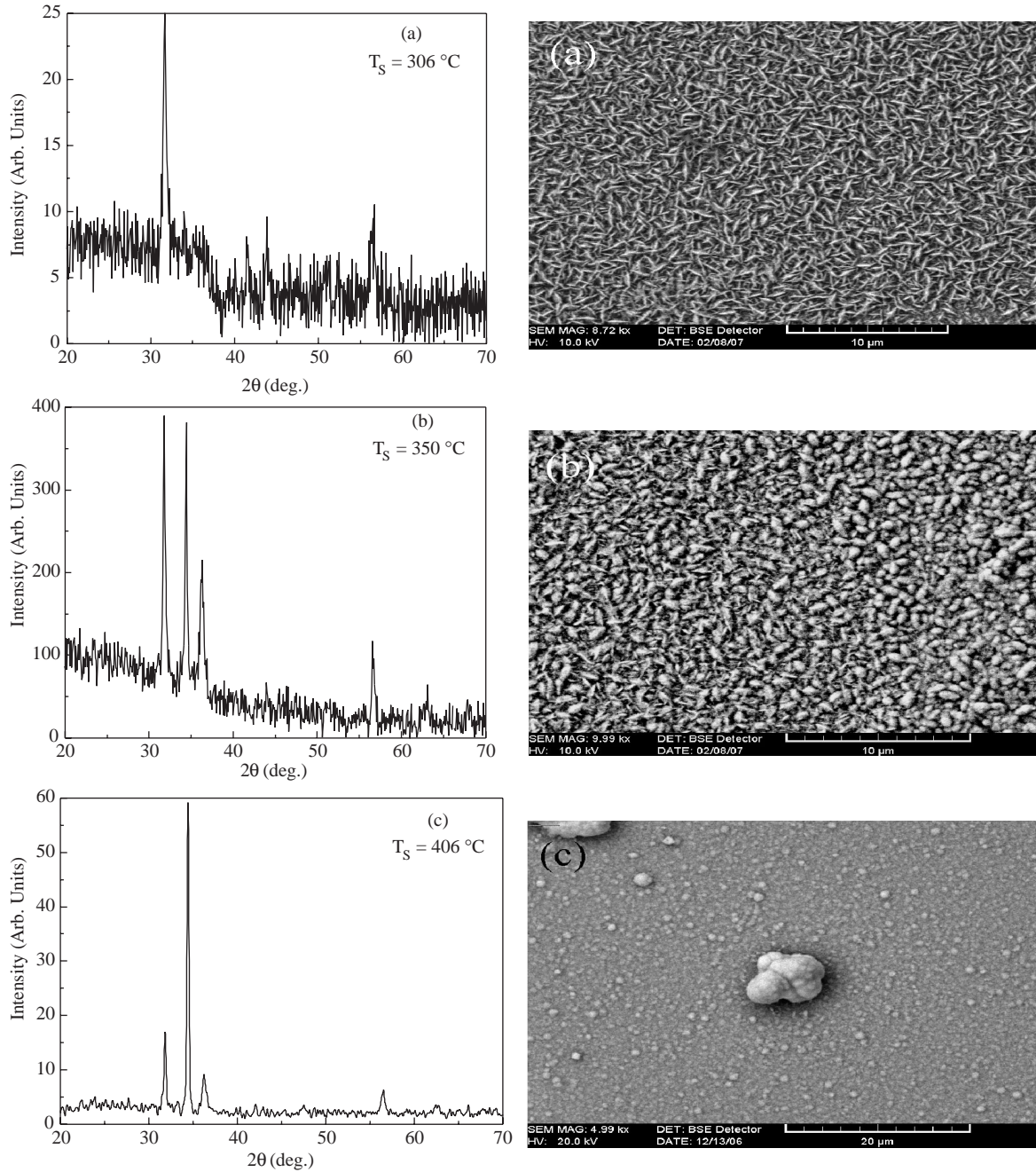


**Figure 5.** X-ray diffraction (XRD) and secondary electron micrographs (SEM) of films obtained from zinc acetate dihydrate solution by USP technique on glass substrate: (a)  $T_S = 306$  °C; (b)  $T_S = 350$  °C; and (c)  $T_S = 406$  °C.

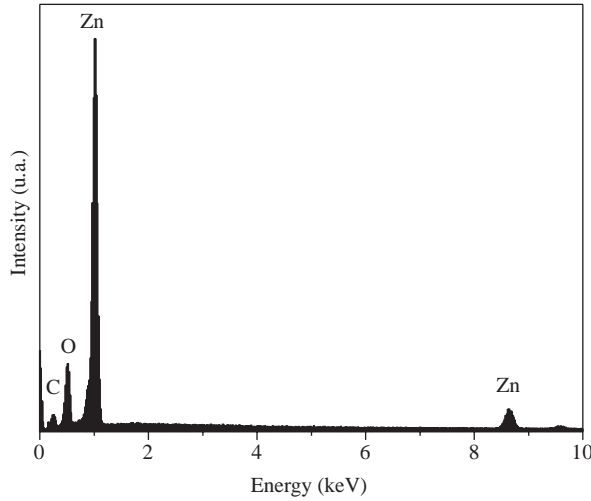
These films show different morphology of surface grains, which are dependent on the deposition temperature. The growth rate and thickness of ZnO thin films deposited on glass substrate at different temperatures are summarized in Table 2. The thicknesses of the films grown at 397 °C and above were on the order of  $\geq 367$  nm, while the films grown below 348 °C were on the order of  $\leq 250$  nm thick.

**Table 2.** Growth rate and thickness of ZnO thin films deposited on glass substrate at different temperatures.

Substrate temperature (°C)	Growth rate (nm/min)	Thickness (nm)
306	4.90	147
330	6.70	201
348	8.33	250
360	9.40	282
397	12.23	367
406	12.60	378
415	13.00	390

As the film thickness decreased, the background increased due to interactions of the X-rays with the underlying amorphous substrate material (see Figure 5, XRD patterns). Though the films are all visually alike, i.e. mirror smooth, the nature of their morphology is quite different. Namely, the geometry of the aggregates grown at lower temperatures ( $< 348$  °C) appears to be lenticular-like, whereas those grown at higher temperatures ( $> 390$  °C) become circular grains. The observation agrees with what is detected from the data of X-ray analysis, as shown by the diffraction spectra in Figure 5. The increasing of the substrate temperature is likely to drive the modification of the grain boundary configuration during growth, which accompanies the appearance of new crystal grains.

Figure 6 shows EDX analysis of the ZnO thin films deposited at  $T_S = 394$  °C. EDX indicates that the products consist of zinc and oxygen elements. The level of carbon contamination detected in the films deposited at 394 °C is 2.5 at.%.


**Figure 6.** EDX analysis of ZnO thin films deposited at  $T_S = 394$  °C.

The crystallite size  $D$  of the samples was estimated using the Scherrer formula [19]

$$D = \frac{0.94 \lambda}{B \cos \theta_B},$$

where  $\lambda$ ,  $\theta_B$  and  $B$  were the X-ray wavelength (1.54056 Å), Bragg diffraction angle and line width at half-maximum, respectively. The crystallite sizes of the films deposited on glass substrate at  $T_S = 330$ , 360 and 397 °C was found to be 31, 34 and 37 nm, respectively.

The band gaps of these films are determined by means of a graphical method from the absorption coefficient derived from the transmittance data. The coefficient of absorption ( $\alpha$ ) can be calculated from



the relation [20]

$$\alpha(\lambda) = t^{-1} \ln\left(\frac{1}{T}\right),$$

where  $T$  is the transmittance,  $t$  the thickness of the thin film and  $\lambda$  the wavelength. The coefficient of absorption over the threshold of fundamental absorption follows a dependency  $\alpha h\nu = A(h\nu - E_g)^n$ , where  $A$  is a constant,  $h$  is the Planck's constant,  $\nu$  is the photon frequency,  $E_g$  is the optical band gap and  $n$  is  $1/2$  for direct semiconductor. The direct band gap of the ZnO films was evaluated by extrapolating the straight line part of the curves  $(\alpha h\nu)^2 = 0$  as shown in Figure 7. The calculated values of band gap  $E_g$  was found to be 3.26, 3.22 and 3.21 eV for the films deposited at 330, 360 and 397 °C, respectively. The band gap values of this study are in good agreement with the band gap values as reported by many earlier workers on ZnO thin films [18, 21, 22]. Films deposited at higher substrate temperatures are found to have lower band gap. It is well known that the ZnO band gap is particularly sensitive to small changes in carrier concentration, grain boundary configuration, and film stress [23, 24].

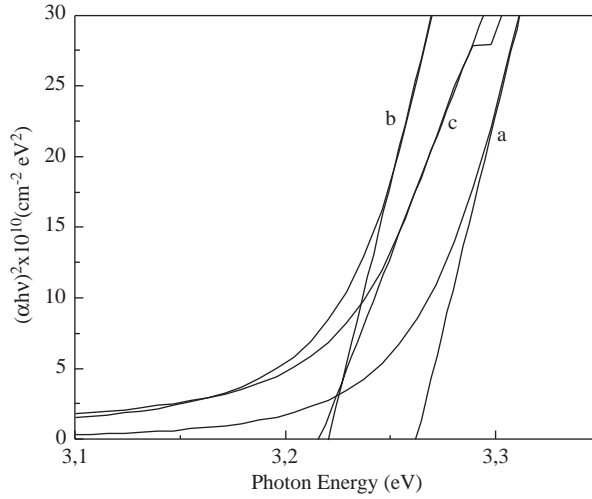


**Figure 7.** Optical band gap of ZnO thin films deposited on glass at (a)  $T_S = 330$  °C, (b)  $T_S = 360$  °C and (c)  $T_S = 397$  °C.

The decrease of band gap with the increase of substrate temperature is likely to be attributed to an increase of crystallite size and a modification of the grain boundary configuration during growth.

## 4. Conclusion

Undoped ZnO films were deposited by USP technique using zinc acetate dihydrate dissolved in methanol, ethanol and deionized water, within the substrate temperature range 140 °C-434 °C. A thermodynamic analysis for the growth of ZnO thin films from zinc acetate and water vapor has been made. The calculations performed in this study indicate that efficient deposition of ZnO thin films by USP is feasible using zinc acetate dihydrate precursors. As reported in the literature, this work demonstrates that water content is necessary to efficiently utilize zinc acetate dihydrate precursors for depositing ZnO with USP. It was seen that the orientation changed with a temperature increase. ZnO Films with different textures were obtained depending on the growth parameters. Specific preparation conditions to obtain films having the (1 0 0) or (0 0 2) orientation only were found. The optical measurements reveal that films have a maximum transmittance of about 90% and a direct band gap of 3.26 eV.

## References

- [1] K. Hara, T. Horiguchi, T. Kinoshita, K. Sayama, H. Sugihara and H. Arakawa, *Sol. Energy Mater. Sol. Cells*, **64**, (2000), 115.
- [2] S. C. Minne, S. R. Manalis, and C. F. Quate, *Appl. Phys. Lett.*, **67**, (1995), 3918.
- [3] T. Makino, C. H. Chia, T. T. Nguen, Y. Segawa, M. Kawasaki, A. Ohtomo, K. Tamura and H. Koinuma, *Appl. Phys. Lett.*, **77**, (2000), 1632.
- [4] D. C. Look, *Mater. Sci. Eng. B*, **80**, (2001), 383.
- [5] M. Tammenmaa, T. Koskinen, L. Hiltunen, L. Ninisto, M. Leskela, *Thin Solid Films*, **24**, (1985), 125.
- [6] J. S. Kim, H. A. Marzouk, P. J. Reucroft and C. E. Hamrin Jr., *Thin Solid Films*, **217**, (1992), 133.
- [7] N. Koga, H. Tanaka, *Thermochimica Acta*, **303**, (1997), 69.
- [8] Hyo-Won Suh, Gil-Young Kim, Yeon-Sik Jung, Won-Kook Choi and Dongjin Byun, *J. Appl. Phys.*, **97**, (2005), 044305.
- [9] T. Aarii, A. Kishi, *Thermochimica Acta*, **400**, (2003), 175.
- [10] Ko Park Sang-Hee, Yong Eui Lee, *J. mater. sci.*, **39**, (2004), 2195.
- [11] J. Hu, R. G. Gordon, *J. Appl. Phys.*, **71**, (1992), 880.
- [12] F. S. Hickernell, *IEEE. Trans. Sonics and Ultrasonics*, SU-**32**, (1985), 621.
- [13] S. Glasstone and D. Lewis, *Elements of Physical Chemistry* (2nd edition), The Macmillan Press Ltd., (New Delhi, 1983), pp. 316.
- [14] D. R. Lide (Ed.), *Handbook of Chemistry and Physics*, 87nd edition, CRC Press, Boca Raton, 2006/2007, pp. 5-2/5-3/5-13/5-16/5-22/5-50/ 5-57/58.
- [15] D. R. Lide (Ed.), *Handbook of Chemistry and Physics*, 61nd edition, CRC Press, Boca Raton, 1980/1981, p. D-77.
- [16] NIST database, <http://www.webbook.nist.gov/chemistry/>.
- [17] Z. N. Prozorovskaya, I. V. Arkhangel'skii, C. A. Castillo, *Zhur. Neorg. Khim.*, **29**, (1984), 1042.
- [18] G. L. Mar, P. Y. Timbrell, and R. N. Lamb, *Chem. Mater.*, **7**, (1995), 1890.
- [19] B. D. Cullity, *Elements of X-ray Diffraction*, 2<sup>nd</sup> ed.; Addison-Wesley: Reading, MA; 1978, p. 102.
- [20] S. T. Tan, B. J. Chen, X. W. Sun, W. J. Fan, H. S. Kwok, X. H. Zhang and S. J. Chua, *J. Appl. Phys.*, **98**, (2005), 013505.
- [21] Kyu-Seog Hwang, Ju-Hyun Jeong, Young-Sun Jeon, Kyung-Ok Jeon and Byung-Hoon Kim, *Ceramics International*, **33**, (2007), 505.
- [22] D. Zaouk, Y. Zaatar, R. Asmar, J. Jabbour, *Microelectronics Journal*, **37**, (2006), 1276.
- [23] V. Srikant, D. R. Clarke, *J. Mater. Res.*, **12**, (1997), 1425.
- [24] V. Srikant, D. R. Clarke, *J. Appl. Phys.*, **83**, (1998), 5447.